Journal of Materials Chemistry A

Accepted Manuscript

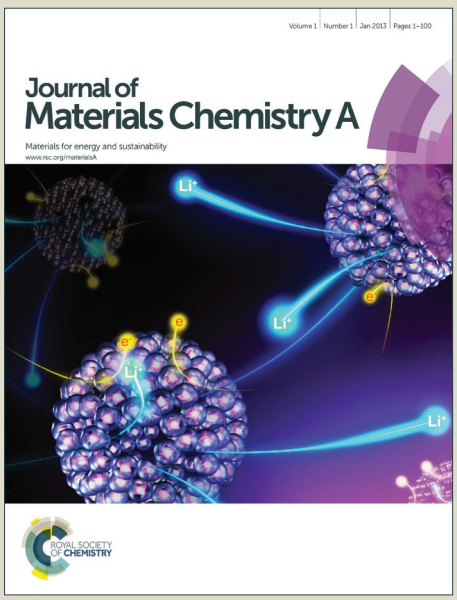

ROYAL SOCIETY OF CHEMISTRY

www.rsc.org/materialsA

Journal of Materials Chemistry A RSCPublishing

ARTICLE

Multilayer composite microcapsule synthesized by Pickering emulsion templates and its application in self-healing coating

Huan Yi, Yu Yang, Xiaoyu Gu, Jian Huang and Chaoyang Wang*

Cite this: DOI: 10.1039/xoxxoooooox

Received ooth January 2012,
Accepted ooth January 2012

DOI: 10.1039/xoxxoooooox

www.rsc.org/

Multilayer composite microcapsules, richly and efficiently loaded with healing reagents (Isophorone diisocyanate, IPDI), are prepared based on lignin nanoparticle-stabilized oil-in-water (O/W) Pickering emulsion templates. The size control of the microcapsules is conducted by varying the lignin content and oil-water volume ratio in Pickering emulsions. With scanning electron microscope (SEM) and optical microscope (OM), the resulting microcapsules show spherical shape, ideal structure of rough outer surface and smooth inner surface, shell thickness of 4.5 μm and mean diameter of 40-117 μm. Fourier transform infrared spectra (FTIR) and Thermal gravimetric analysis (TGA) indicate extraordinary characteristics of the capsules: core fractions of 81.1 wt.%, excellent thermal stability with initial evaporating temperature of IPDI elevated for 72 °C, firm durability among aqueous solution-submersion and air-exposure with mass loss about 9.7 wt.% after four days submersion or two weeks exposure. Furthermore, the microcapsules are embedded into epoxy coatings for applying this technology into anticorrosive polymer coatings. Investigated by brine-submersion corrosion-accelerating test, the self-healing microcapsules-incorporated epoxy coatings on steel plates demonstrate good dispersibility of capsules in coatings and favourable anticorrosive effects.

Introduction

Capsule-based self-healing materials have attracted increasing attention and been extensively investigated,[1-7] notably since the first generation repairing system reported by White et al.[8] more than a decade ago. Meanwhile, by applying this technology into coating industry, capsule-based self-healing materials open up a prosperous field of smart coatings that can give instant feedback to external signal, renovate themselves autonomously and significantly prolong the service life.[9-14] As researched in previous studies,[15,16] to provide these self-healing functions, active healing reagents are required to be wrapped in micro-capsules before being incorporated into self-healing coatings. Upon crack damage of the self-healing coating, the embedded microcapsules simultaneously rupture, release the encapsulated healing reagents, and refill the cracked area.[17] Therefore, self-healing microcapsule is demanded to possess several features, which contain high encapsulation efficiency, well protective capability for core material and rapid responsiveness towards ambient hazards and so on, since it plays an important role in repairing performance of capsule-based intelligent materials.[18] Moreover, for its future application in coating industry, quick, mass production of the capsule is also of great importance.

Various approaches to fabricate self-healing microcapsule have been widely reported, including layer-by-layer assembly technique,[19,20] self-assembly of amphiphilic block copolymers into spherically closed structure by reversible addition fragmentation chain transfer (RAFT) polymerization,[21] solvent evaporation method,[22] coacervation,[23] microfluidic technique[24-27]. Nevertheless, when the wrapped core material comes to be liquid isophorone diisocyanate (IPDI), the capsulation technology is severely restricted, because IPDI is a highly reactive healing reagent for one-component catalyst-free self-healing system. Once outflowed from microcapsule, IPDI can effectively react with water and moisture (main factors for the corrosion of steel) in ambient environment, form solid material and effectively prevent the substrate from corrosive attack. Yang et al.[28] made the first successful attempt of IPDI encapsulation via interfacial polymerization of polyurethane (PU), and there were three other literatures that had reported the IPDI encapsulation in microcapsule till now.[28-30] However, numerous hardships, including insufficient IPDI loading capability and efficiency, undesirable shape and inner/outer shell morphology of capsule, difficulty of being facilely synthesised in large quantity, etc., still remain to be solved.

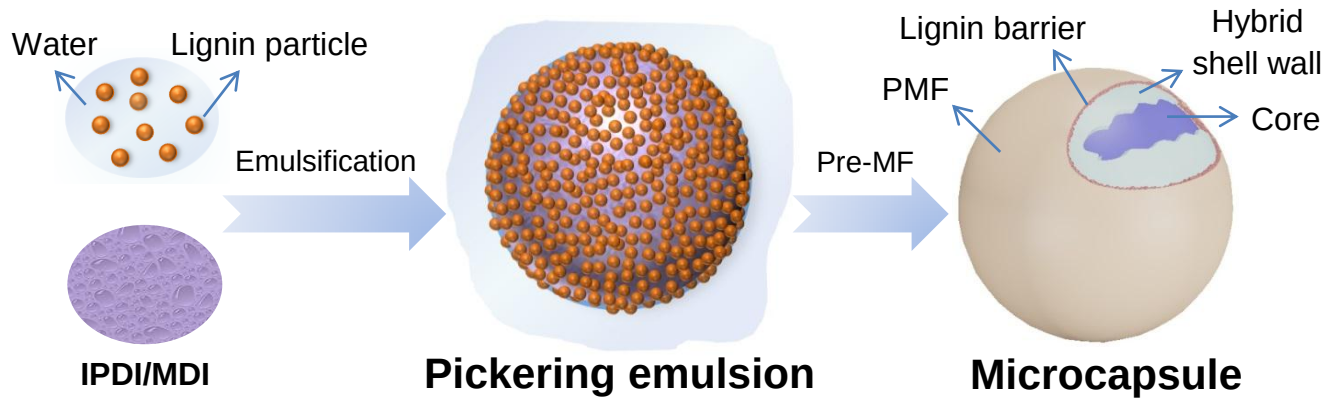

Fig. 1. Schematic for the synthesis process of multilayer composite microcapsules loaded with healing agents based on Pickering emulsion templates.

To complete these breakthroughs, microcapsule prepared based on oil-in-water (O/W) Pickering emulsion template is firstly applied in the capsulation of IPDI. Previous work focused on traditional molecular surfactant, but it provides insufficient stability to protect emulsion droplets from demulsification in the formation process of microcapsules. In contrast, Pickering emulsions are stabilized by adsorption of solid particles at the oil-water interface,[31] which can greatly enhance the stability of emulsion, reduce the loss of core material, and guarantee the high encapsulation efficiency.[32-34] At the same time, the barrier constructed by the self-assembling of solid particles can serve as framework to form more strengthened shell wall, reinforce the resistance of capsule and preserve core materials from deactivation of ambient hazards.[35,36] Moreover, various particle stabilizers retained in shell can introduce multiple functions (e.g., pH sensitiveness, magnetic responsiveness) into microcapsules, which is conducive to develop the promising application of microcapsules in intelligent materials.[9,37]

Here, we present a facile and efficient method for the synthesis of IPDI-loaded multilayer composite microcapsules with outstanding thermal and solution resistance based on O/W Pickering emulsion template. Alkaline lignin is chosen as emulsion stabilizer for its inexpensiveness and abundance, which made it more available for this method further applying in practical application.[38] As the schematic plot shown in **Fig. 1**, O/W Pickering emulsion stabilized by lignin particles is prepared, and oil phase is the mixture of IPDI and diphenyl methane diisocyanate (MDI). MDI, aromatic diisocyanate, is much more reactive than IPDI (aliphatic isocyanate) towards amines or alcoholic molecules.[39] So, isocyanate groups of MDI can preemptively react with hydroxyls of lignin or water at the interface of emulsion droplet and form a thin PU membrane. Then, microcapsules are formed by interfacial polymerization and in situ polymerization of melamine formaldehyde pre-polymer (pre-MF). Moreover, to research self-repairing effect of the obtained microcapsule, self-healing coating is prepared by incorporating the IPDI-loaded microcapsules into epoxy resin, and it is demonstrated to be effectively anticorrosive by brine-submersion corrosion-accelerating test.

Experimental Section

Materials

Lignin, the Pickering emulsion stabilizer, was obtained from furfural residues by Kraft pulping process. Polyvinyl alcohol (PVA AH-26, polymerization degree of 2600, alcoholysis degree of 97-98.8%, viscosity of 58-66 mPa·s) served as emulsion dispersant, was purchased from Sinopharm Chemical Reagent Beijing Co., Ltd. Isophorone diisocyanate (IPDI) worked as healing reagent was bought from Aladdin Industrial Corporation. Modified Diphenyl Methane Diisocyanate (MDI, Lupranate MM103C) was supplied by BASF, China. Ammonia solution and Triethanolamine (TEA) were supplied by Chinasun Specialty Products Co., Ltd. Hydrochloric acid (HCl) was supplied by Guangzhou Chemical Factory and used without purification. Melamine and 37.0 wt% formaldehyde, for the preparation of prepolymer of melamine-formaldehyde (pre-MF), were purchased from Shanghai Lingfeng Chemical Reagent Co. Ltd. and Guangzhou Donghong Chemical Factory respectively. Epoxy resin (EF200, Guangzhou LAPO Fine Chemical Co. Ltd.) acted as matrix material of self-healing coating. Ethanol (Guangzhou Chemical Factory) was used for degreasing of steel plates. Sodium chloride (NaCl), employed in salt-immersion corrosion experiment, was provided by Shanghai Richjoint Chemical Reagent Co. Ltd. Acetone was purchased from Guangzhou Donghong Chemical Factory for extraction of IPDI in microcapsules. All chemicals are used as received unless otherwise specified. Deionized (DI) water in all experiments was purified with Millipore (MA, USA) purification equipment by deionization and filtration to a resistivity above 18.0 MΩ cm.

Lignin Stabilized Oil-in-Water Pickering Emulsions

Pickering emulsions with different lignin contents and oil-water volume ratios were fabricated as listed in **Table 1**. A typical emulsion of sample 3 was prepared by following steps. Firstly, 15 mg lignin was added into 5 mL DI water. The pH of Lignin dispersion was adjusted to 10-11 by ammonia solution (37%), and lignin powder was absolutely dissolved. Then, the pH of

Sample	Water phase		Oil phase		O/W volume ratio	Droplets size(μm)
	Water (mL)	Lignin (wt.%)	IPDI (mL)	MDI (mL)		
1	5	1.0	4	1	1 : 1	42.1 ± 17.1
2	5	0.5	4	1	1 : 1	68.3 ± 18.9
3	5	0.3	4	1	1 : 1	82.6 ± 21.5
4	5	0.1	4	1	1 : 1	94.3 ± 26.0
5	5	0.05	4	1	1 : 1	102.3 ± 28.4
6	5	0.01	4	1	1 : 1	114.5 ± 36.7
7	5	0.3	8	2	2 : 1	127.8 ± 43.6
8	5	0.3	6	2	1.6 : 1	109.4 ± 29.7
9	5	0.3	4	2	1.2 : 1	87.1 ± 28.2
10	5	0.3	3	1	0.8 : 1	76.4 ± 23.6
11	5	0.3	1.5	0.5	0.4 : 1	63.9 ± 19.2
12	5	0.3	0.4	0.1	0.1 : 1	27.4 ± 12.8

Table 1. Parameters of lignin stabilized O/W Pickering emulsion templates with different lignin contents (sample 1-6), oil-water volume ratio (sample 7-12) and mean droplets size in each samples.

Lignin solution was set to 2-3 with HCl, lignin particles formed and dispersed in the solution. Finally, the mixture of 4 mL IPDI and 1 mL MDI was added into the lignin particle suspension. The O/W Pickering emulsion was formed after heavily shaking by hand for 3 min.

Pre-MF

Pre-MF was synthesized with the method reported by Meng et al.[40] with some amendment. 0.03 mol melamine, 0.1 mol formaldehyde, and 8 mL water were mixed in a 50 mL three-neck flask with a magnetic stirrer. The pH of the mixture was set to 8.5-9.0 by adding TEA. In the meanwhile, the system was heated to 60 ^{o}C. After constant agitating for 30 min, the pre-MF solution was formed and remained on standby.

Composite multilayer microcapsules loaded with healing agent

A 250 mL three-neck flask with 0.1 wt% PVA solution (50 mL) was heated to 50 ^{o}C at a heating rate of 10 ^{o}C min^{-1}, the temperature was then stabilized in 50 ^{o}C, and the system was stirred constantly till the end of reaction (400 rpm). Then, the above fabricated Pre-MF was poured into the PVA solution, and the pH of the obtained solution was adjusted to 2-3 with HCl. After 1 min, the prepared oil-in-water Pickering emulsion was added dropwise into the three-neck flack with dropper. The reaction was conducted for 2 h, and the IPDI-loaded micro-capsules were efficiently formed. The obtained microcapsules were washed for three times with DI water to remove the free PMF particles suspended in water. Finally, the microcapsules were air-dried at room temperature for 24 h and stored for further experiments.

Self-healing coatings on steel plate

Microcapsules containing self-healing agents were dispersed into epoxy resin at room temperature to prepare the self-healing coatings, followed by mixing hardener into the composites (Epoxy/hardener/microcapsule mass ratio: 100/25/15). The mixtures were degassed in vacuum for 15 min. Steel plates (size, 10×10 cm^2) buffed off by sandpaper (04#) and degreased with ethanol were employed as substrates. The prepared self-healing composites were applied to the dried steel plates with layer thickness of about 500 μm and cured for 24 h at room temperature. Control samples were coated by pure epoxy-hardener system with same thickness and size, and prepared with same manners for comparison.

After cured, the self-healing coatings and control samples were scratched manually with scalpel, and all specimens were immersed in NaCl solution (10 wt.%) for 120 h. The optical photographs and electrochemical impedance spectroscopy (EIS) measurements were taken to research the comprehensive anticorrosion performances of self-healing coatings.

Characterizations

Optical Microscopy (OM): Pickering emulsions with different lignin contents and oil-water ratios, multilayer IPDI-containing microcapsules and core materials released from microcapsules after scratching on self-healing epoxy coating were recorded by an Axiolab Polarizing Microscope (Carl Zeiss, Germany) equipped with a camera.

Scanning Electron Microscopy (SEM): The appearance, inner/outer surface morphology, shell wall thickness of microcapsules and fracture surfaces of self-healing epoxy coatings were analysed with a Zeiss EVO 18 scanning electron microscope operating at 10 kV.

Microcapsule Size Analysis: The average diameter and size distribution of microcapsules were summarized from data of about 200 measurements from OM images and analysed by Nano Measurer 1.2.

Fourier Transform Infrared spectra (FTIR): FTIR spectra of IPDI, microcapsules and their shell were performed with a German Vector-33 IR instrument. The shell was obtained by following procedure. Small amount of microcapsules were crushed in agate mortar. Then, the capsule powders were transferred into a beaker, washed with acetone to dissolve the IPDI in powder, and filtrated. This process was repeated for three times. Finally, the resulted capsule shell was dried in vacuum.

Total IPDI Encapsulation Efficiency: Acetone extraction was applied to measure the IPDI-encapsulation efficiency of microcapsules. Firstly, microcapsules weighed as W_1 g were synthesised from Pickering emulsion template with W_2 g IPDI. Thereafter, the microcapsules were grinded in an agate mortar with a pestle and washed with acetone. The above suspension was centrifuged at a speed of 10000 rpm for 3 min, and the precipitation was collected. These processes were repeated for three times. The obtained sediment was dried in vacuum oven at 60 ^{o}C, and afterwards weighed as W_3 g. Finally, the total IPDI encapsulation efficiency (η) of the microcapsules was calculated by:

$$\eta = [(W_1 - W_3)/W_2] \times 100\%$$

Thermal Gravimetric Analysis (TGA): TGA of IPDI, shell and microcapsules with different lignin contents were

performed with a NETZSCH TG 209F3 instrument. Typical experiment process of TGA was as follow: 3-6 mg samples were placed on aluminium oxide crucible neatly and heated from 40 to 600 ^{o}C at a heating rate of 10 ^{o}C min^{-1} under nitrogen atmosphere.

In addition, resistant properties of the microcapsules towards air exposure and aqueous immersion were researched by TGA.

Electrochemical impedance spectroscopy (EIS): EIS was conducted by a CHI660E electrochemical workstation (Shanghai Chinstru Co. Ltd., China) in a conventional three electrode cell (open to air) containing working electrodes (common coatings and self-healing coatings coated specimens), a platinum filament as the counter electrode and saturated calomel electrode as the reference electrode at 25 ℃. EIS measurements were performed using an AC signal with an amplitude perturbation of 10 mV at open circuit potential in the frequency range of 10^{5} Hz to 10^{-2} Hz.

All experiments were performed in triplicate to ensure the data accuracy, and the average values were calculated.

Results and discussion

Preparation and characteristics of composite microcapsules

Microcapsules, based on O/W Pickering emulsion template, were synthesised by following the procedures displayed in Fig. 1. Pickering emulsion, in which the solid particles adsorbed on oil-water interface in replace of the surfactants in traditional emulsion, was remarkably stable to protect droplets from aggregating.[41,42] It could be facilely and efficiently prepared, and had been applied in a vast range of advanced materials.[43-45]

Pickering emulsion templates: Here lignin was employed as Pickering emulsion stabilizer, not only for its inexpensiveness, eco-friendliness but also because there were lots of active hydroxyl groups in the chemical structure of lignin (Figure. S1), which could react with isocyanate groups in oil phase and reinforced the stability of emulsions. While alkaline lignin was insoluble and aggregated on water (Fig. S2a), it was required to prepare lignin particle suspensions before fabricating Pickering emulsion. Lignin dissolved in water when pH value was adjusted to 10-11 by ammonia solution. Then, it precipitated out as dispersed particles when pH value was regulated to 2-3 with HCl (Fig. S2b, c) and formed lignin particle suspension.

Pickering emulsion was synthesised by adding oil phase (mixture of IPDI and MDI) into lignin suspension with heavily shaking by hand. Stable Pickering emulsion could be facilely fabricated by hand shaken for three minutes since the energy needed for the formation of a specific Pickering emulsion had its lower bounds. Once the energy provided was sufficient to form this Pickering emulsion, the size and morphology of emulsion droplets were mainly related to the synthesis parameters of emulsion, and would not extensively change with small energy difference made by hand shaken method (Fig. S3). Moreover, the time-stability of Pickering emulsion was severely related to the reactivity of oil phase with water. In this experiment, the oil phase was the combination of highly active reagents, IPDI and MDI. As the OM images shown in Fig. S4, the emulsion started to demulsify after standing for about 3 h, and became invalid about 6 h.

Lignin particles in Pickering emulsions rapidly assembled around oil droplets and formed a steady solid barrier between oil and water phase.[43] Isocyanate groups of MDI exhibited much higher reactivity than those of IPDI because of the electron withdrawing effect of benzene ring. Thus, by interfacial polymerization, MDI in oil phase promptly reacted with water and lignin at the interface of droplets, formed thin PU membrane and further strengthened the encapsulation of healing agents. By comparing the OM images of Pickering emulsion with or without MDI in Fig. S5, MDI could also be clearly demonstrated to act as the enhancer in emulsion. In addition, the influence of varying ratios of IPDI and MDI on the Pickering emulsions and obtained microcapsules was further researched by OM and SEM. As the OM images displayed in Fig. S6, the morphology of Pickering emulsions with different IPDI-MDI volume ratios in oil phase were in stark contrast with each other. The emulsion droplets presented in Fig. S6a kept spherical overall with considerable thin "outer ring" around droplets, while droplets in Fig. S6c were grotesque in shape with thick "outer ring", which meant insufficient stability of this emulsion. Meanwhile, microcapsules synthesized with different Pickering emulsions are demonstrated by SEM images in Fig. S6. With the increasing amount of MDI in oil phase, the obtained products gradually varied from neat spherical capsule to disorderly cross-linked structure with random shape.

The exceedingly high activity of isocyanate groups in MDI and its quick reaction with amine could be the reason for these phenomena. Once mixed in water phase, the isocyanate groups

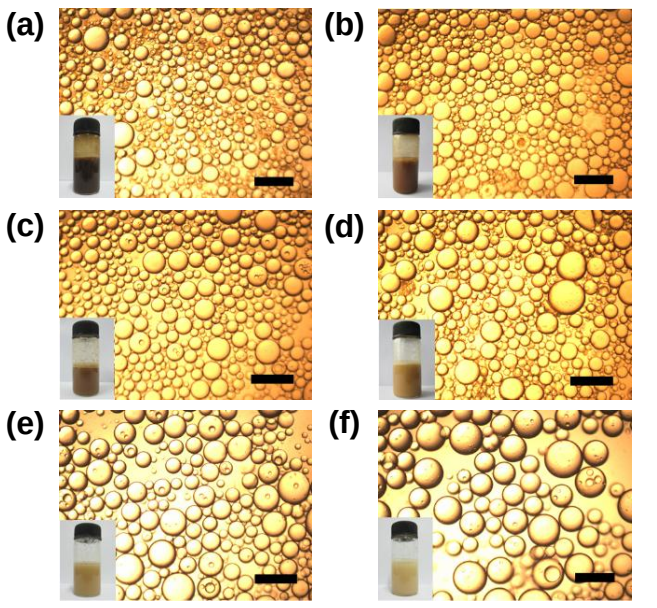

Fig. 2. OM images and photos of Pickering emulsions with different lignin content. (a) 1.0 wt.%, (b) 0.5 wt.%, (c) 0.3 wt.%, (d) 0.1 wt.%, (e) 0.05 wt.%, (f) 0.01 wt.%. All scale bars are 200 μm.

of MDI would reach oil-water interface massively, and react with the hydroxyl groups of water and lignin, which leaded to the thick "outer ring" and bubbles in oil phase. Thus, MDI could not keep stable when encapsulated, and it rapidly cross-linked with melamine during the preparation of microcapsules. TGA curves in Fig. S7 proved that MDI was not encapsulated in cores but formed shell materials in this experiment.

Herein, the size control of the microcapsules was conducted by varying the lignin content and oil-water volume ratio in Pickering emulsions. As shown in **Fig. 2**, droplets in Pickering emulsions exhibited spherical shape, and even kept stable in a considerably low mass ratio (0.01 wt.%). The average diameter and size distribution of droplets increased with the reduction of lignin contents, from 42.1±17.1 μm (1.0 wt.%) to 114.5±36.7 μm (0.01 wt.%), which was essential for the control of the size of self-healing microcapsules, and in accord with previous report.[35] On the other hand, the influence of oil-water volume ratios on the size of Pickering emulsion droplets was investigated. From Fig. S8, it could be concluded that mean diameter and size distribution of droplets rose up along with the growing amount of oil phase, from 27.4±12.8 μm (0.1:1) to 127.8±43.6 μm (2.0:1). However, with excessive oil-water volume ratio (more than 2.0:1), Pickering emulsions were not stable enough to establish microcapsule in further reaction, while insufficient would lead to the lack of core material, and the resulted capsule could not be self-healing in its application.[44]

Therefore, we optimized the parameters of Pickering emulsion template as sample 3 (Table 1) for the synthesis of self-healing microcapsules.

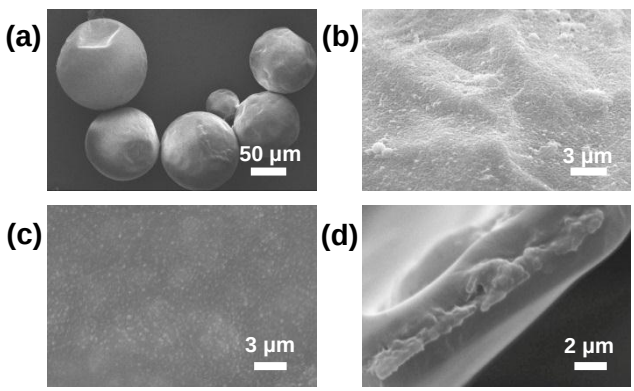

Fig. 3. SEM images of IPDI-loading composite multilayer microcapsules (Sample 3). (a) Spherical shaped microcapsule, morphology of (b) outer Surface and (c) inner surface, (d) cross section of shell.

IPDI-loaed composite multilayer microcapsules: PVA served as surfactant, Pre-MF as shell material, the multilayer microcapsules were prepared with Pickering emulsion template. Pre-MF, water soluble oligomer, could self-crosslink to form MF polymer while pH of the reaction system was adjusted to 2-3, and wrap around the Pickering emulsion droplets. Meanwhile, pre-MF could also react with diisocyanate within oil phase of Pickering emulsion, which generated polyurea as main shell materials by interfacial polymerization. As the SEM images displayed in **Fig. 3**, the obtained microcapsules showed spherical shape, smooth inner surface and rough outer surface, which were beneficial to out-flowing of core material and dispersibility of microcapsule in epoxy coating. This appearance difference was caused by diverse reaction conditions: inner surface was formed by interfacial polymerization between isocyanate groups in oil phase and pre-MF in water phase, and formed tightly cross-linked polyurea as the main components of shell, while outer surface was PMF wall constructed with in situ polymerization of pre-MF on the surface of microcapsule. Moreover, the cross section of shell in Fig. 3d indicated the multilayer structure of capsule, the inlaying lignin aggregates in shell, and thickness of shell about 4.5 μm and roughly consistent. On the other hand, **Fig. 4** showed the size distribution of capsules synthesised by emulsion sample 3. The approximate size of capsules and emulsion droplets confirmed the constancy and efficiency of emulsion template, and the size control of microcapsules could be facilely conducted by varying the lignin contents in Pickering emulsion, and the mean diameter of microcapsules, similar to the droplets size discussed above, decreased with increasing amount of lignin contents (**Fig. 5**).

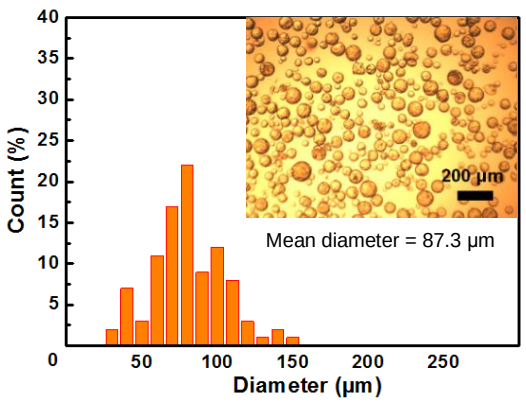

Fig. 4. Mean diameter, size distribution and OM image of microcapsules. The microcapsules were prepared by Pickering emulsion template sample 3.

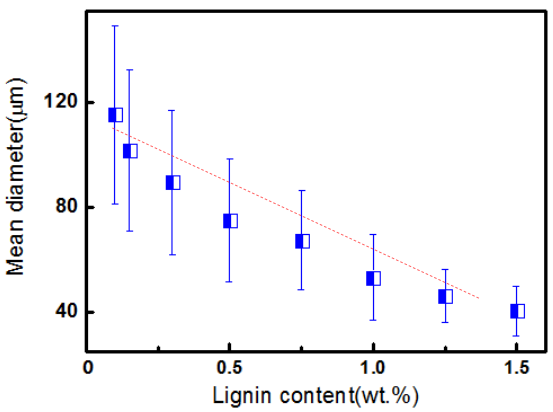

Fig. 5. Decrease in mean diameter of microcapsules with increasing amount of lignin contents in Pickering emulsion template.

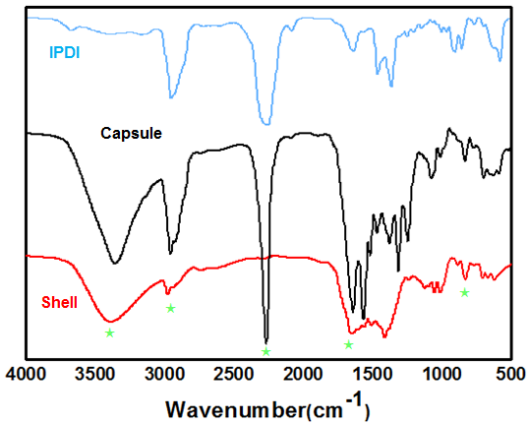

Fig. 6. FTIR spectra of IPDI, the IPDI-containing microcapsule and its shell.

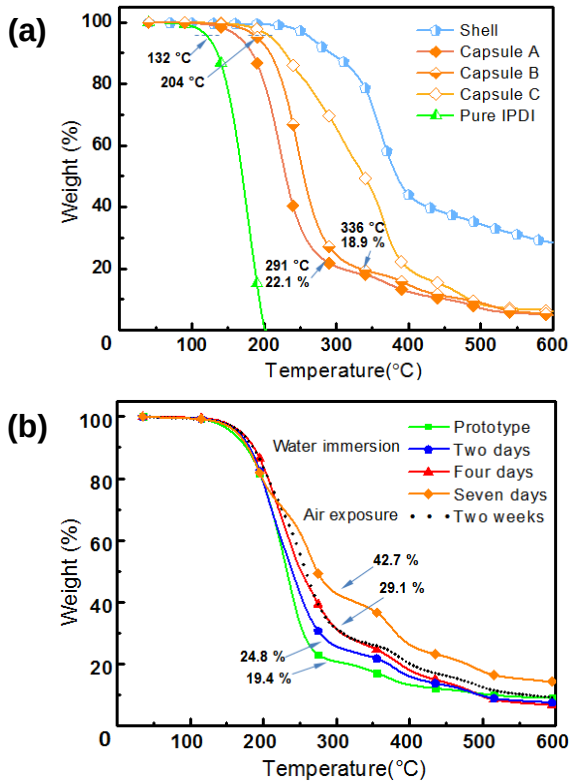

Fig. 7. Characterization of resistant property. (a) TGA curves of IPDI, shell and microcapsules synthesised by Pickering templates with different lignin contents. (A) 0.1 wt.% (B) 0.5 wt.% (C) 2.0 wt.%. (b) TGA curves of microcapsules after immersed in aqueous solution for two days (blue), four days (red), seven days (orange) and exposed in air for two weeks (dotted line). Microcapsules prototype (green) were synthesised from Pickering emulsion template sample 3 (Table 1).

In addition, FTIR spectra of IPDI, the IPDI-loaded microcapsule and its shell were conducted to further reveal the detail components of this novel microcapsule (**Fig. 6**). With wide stretching vibration peaks of N-H at about 3353 cm^{-1}, stretching vibration peaks of aliphatic C-H at 2955 cm^{-1}, characteristic peaks of C=O and N-H in carbamido group at 1642 and 1503 cm^{-1} existed in spectrum of capsule and shell, polyurea and PU could be proved to be the main component of shell. PU wall was firstly established by isocyanate-hydroxyl chemistry as discussed above, while polyurea wall was constructed by interfacial polymerization between diisocyanate (-NCO) and melamine ($-NH_2$). The outer PMF wall could be manifested with representative peaks as stretching vibration of C=N at 1366-1556 cm^{-1} and stretching of triazine ring at 820cm^{-1}. Typical peak of CH_2O-C at 1037 cm^{-1} in shell confirmed the existence of alkali lignin. More importantly, the intensive absorption peak of stretching vibration of C=O in isocyanate group appeared at about 2262 cm^{-1} in both spectra of IPDI and microcapsule, which firmly proved that IPDI, served as healing agent, was efficiently encapsulated in the composite multilayer microcapsule.

Furthermore, as a container of active healing reagent, the preservative capability of the microcapsule was vital for its practical application. So, TGA of IPDI and microcapsules (**Fig. 7**) were performed to measure the thermal resistance of microcapsules. As shown in Fig. 7a, vaporization temperature (defined as 5 wt.% mass loss) of IPDI was 132 °C, while the IPDI encapsulated in microcapsules exhibited remarkable thermal stability by elevating the temperature to 204 °C (capsule B). The reinforcement could be attributed to the multilayer barrier formed with PU, PMF and inlaid lignin aggregates, which firmly hindered IPDI from permeation. TGA curves also showed that IPDI was richly encapsulated in microcapsule with the mass ratio reached about 81.1 wt.%. Along with the total IPDI encapsulation efficiency (η) of about 87% and little IPDI reacted with pre-MF, it could be confirmed that the IPDI in Pickering emulsion template was preserved in microcapsules with high efficiency. Moreover, in comparison with the TGA curves of shell and capsule A, B, C (Fig. 7a), it was discovered that capsules with more lignin content in Pickering emulsion had relatively better thermal stability and lower core fraction (as capsule C, and extreme case as shell). It could be illuminated as follow. On one hand, more lignin particles massively aggregated around the oil droplet led to smaller droplet size and internal volume of capsules (as discussed above), and decreased the core fraction in capsules. On the other hand, more lignin particles could react with more isocyanates in oil phase and established stronger shell wall of PU, and further prevented the IPDI from vaporizing. More interestingly, the capsule B owned both two advantages towards A. It might be explained that Pickering emulsion template with less lignin content (A: 0.1 wt.%) was less stable during the preparation of capsules, and IPDI leaked out from droplet, which resulted in the reduction of both core fraction and thermal stability.

To further research the resistant property of this IPDI-loaded multilayer microcapsule, aqueous solution-immersion and air-exposure experiments were conducted. As shown in TGA traces of Figure 7b, the weight loss of core fraction in microcapsules was only 5.4 wt.% after immersed for two days (tested after drying), indicating good solvent stability of microcapsules. While sufficient core materials were also essential for the application of capsules in self-healing coating, it was surveyed that capsules were still available for anticorrosive function after immersed for four days (core fraction about 70.9 wt.%). Meanwhile, with the TGA traces in

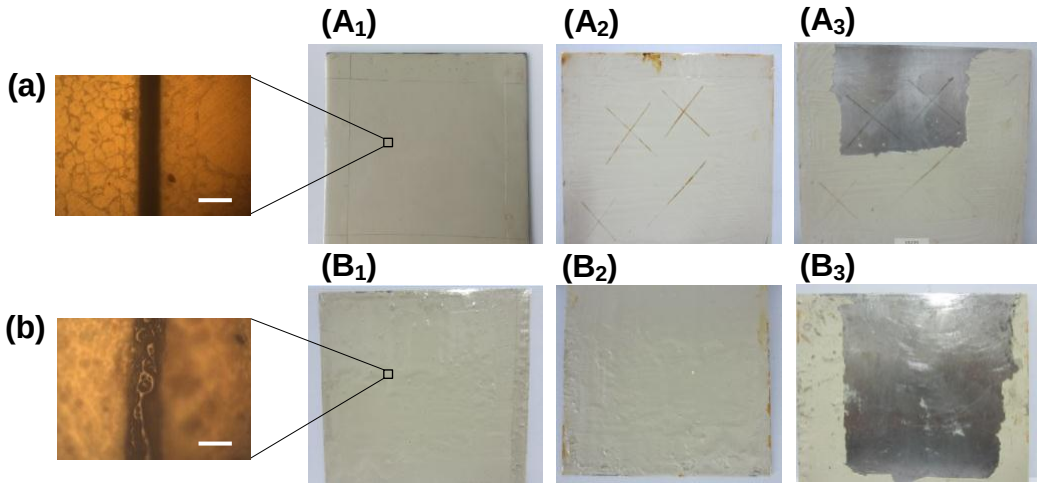

Fig. 8. Brine-submersion corrosive-accelerating test. Photograph of steel plates coated with common coating (Group A) and microcapsule-embedded self-healing coating (Group B): (A1, B1) before, (A2, B2) after submersed in 10 wt.% NaCl solution for 120 h, and (A3) traces of corrosion on steel plate, (B3) anticorrosive performance of self-healing coating on steel plate. OM images of Enlarged view of scratched region on (a) common coating and (b) self-healing coating, the scale bars are 200 μm. The steel plates (10×10 cm2) were submerged in NaCl solution (10 wt.%) for 120 h.

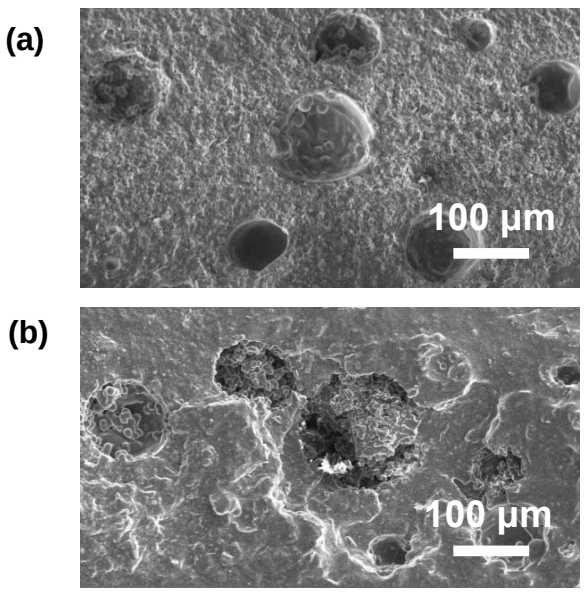

Fig. 9. SEM images of (a) fracture surface rinsed with acetone instantly after flawed, and (b) fracture surface revealed on self-healing coating after self-healed.

Fig 7b, microcapsules, exposed in air for two weeks, demonstrated approximate amount of core effusion as those immersed for four days in aqueous solution. Moreover, capsules, which were immersed in aqueous solution for seven days (Fig. S9 and S10), could still detect the outflowing of active reagents after embedded and cracked in coatings (core fraction about 57.3 wt.%), which provided strong support for its practical application in industry fields.

Anticorrosive performance of the self-healing coating

As an important part of advanced material, the self-healing materials with various repairing approaches had been widely investigated,[48-53] and capsule-based self-healing material with one-part repairing system were of technological importance and owned broad developing prospect.[54-57]

Here, self-healing epoxy coatings applied on refined steel plates (size, 10×10 cm^2) were prepared as stated above, and following by brine-submersion corrosion-accelerating test to investigate the anticorrosive capability of epoxy coatings containing self-healing microcapsules compared with that of common coatings. After completely cured for 24 h, the self-healing coating and control sample were scratched with scalpel at room temperature. Two specimens were then submerged in NaCl solution (10 wt.%) to accelerate the corrosion on steel plate, and taken out to record the corrosion status after 120 h submersion. As shown in **Fig. 8**, the scratched regions on control sample (group A) were severe corroded, several traces of rust could be found on steel plate after the coating being peeled off. However, the steel plate coated with self-healing coating (group B) withstood the erosion of brine, and showed no visual sign of corrosion even after 120 h submersion (Original picture of steel plate after peeling off self-healing coating in Fig S11 clearly revealed the scratch regions).

EIS measurements were conducted to research the comprehensive anticorrosion performances of self-healing coatings. Bode plots in Fig. S12 proved that microcapsules in coatings would not affect impedance of whole electrochemical system, and result in experimental errors. Fig. S13a showed that the steel plates coated self-healing coatings had higher impedance than those coated with common coatings in the process of corrosion. The impedances of coatings with self-healing microcapsules kept relatively stable, while the scratches on all coatings decreased impedance of whole electrochemical system (comparing to Bode plot in Fig S12a). Bode plot in Fig. S13b indicated that the equivalent circuit of self-healing system had an additional RC element in comparison to that of common system. Furthermore, Nyquist plots in Fig. S14 showed the distinct impedance difference of two systems after immersed

for 72 h, and proved the IPDI outflowed from microcapsules effectively slowed down corrosion on steel plate.

From the OM images of scratched regions on two specimens (Fig 8a, b), it could be concluded that the excellent anti-corrosive property of the self-healing coating entirely owed to the embedded IPDI-loaded microcapsules, which released quantities of active reagents at scratched area upon cracked. The outflowed IPDI could react with water or moisture and form PU by isocyanate-hydroxyl chemistry. In this way, the flaws on self-healing coating were repaired automatically, and the corrosion hazard, including salt ions, air, water, were all isolated from the substrate. Thus, the corrosive attack could be forbidden, and steel plates coated with self-healing coatings were prevented from rust.

Furthermore, the fracture surface, rinsed with acetone to remove the healing reagents instantly after flawed (**Fig. 9**a), showed the residual cracked microcapsule embedded in coating. In contrast, the SEM image in Fig. 9b revealed the substance of polymerized healing reagent on fracture surface. It indicated the in situ formation of healed material in cracked region and further confirmed the spontaneous repairing function of IPDI-loaded microcapsules in the self-healing coating.

Conclusions

Multilayer composite microcapsules, richly loaded with IPDI, were synthesised with lignin stabilized O/W Pickering emulsion template by in situ and interfacial polymerization. The size control of microcapsules was deftly conducted by varying the lignin contents and oil-water volume ratio in Pickering emulsion template, and mean diameter scale of capsules was about 40 to 117 μm. The core fraction of microcapsules more than 81 wt.%, along with the total IPDI encapsulation efficiency of 87%, guaranteed the sufficiently preservation of core material in microcapsules. The resulted microcapsule presented spherical shape, rough outer surface and smooth inner surface, and the shell wall of microcapsule inlayed with lignin barrier showed multilayer composite structure and thickness of about 4.5 μm. Meanwhile, owing to the rigid protection of shell wall, the capsule exhibited excellent resistant properties towards harms, including high temperature, moisture and aqueous solution. These outstanding characters of the microcapsule powerfully supported its further application in industrial and environmental fields.

Finally, brine-submersion corrosion-accelerating test were performed to investigate the healing effect of microcapsules in epoxy coating. As a result, the self-healing coating, which was embedded with IPDI-loaded capsules, exhibited remarkable anticorrosive effect on protecting steel plate, and the substrate showed no visual sign of corrosion even after 120 h submersion in NaCl solution (10 wt.%), while the control sample was severely rusted. EIS measurements were also conducted and proved repairing role of microcapsules in self-healing coatings. Meanwhile, the OM and SEM images revealed in fracture region demonstrated that the active reagents, outflowed from microcapsules in coating, polymerized to form solid materials in cracks and stopped the corrosive attack, which was indicative of automatic repairing property and promising potential of this self-healing microcapsule.

Acknowledgements

This work was financially supported by the National Natural Science Foundation of China (21274046 and 21474032) the National Natural Basic Research Program of China (973 Program, 2012CB821500) and the Natural Science Foundation of Guangdong Province (S2012020011057).

Notes and references

Research Institute of Materials Science, South China University of Technology, Guangzhou 510640, China. Fax & Tel: +86-20-2223-6269; E-mail: zhywang@scut.edu.cn.

† Footnotes should appear here. These might include comments relevant to but not central to the matter under discussion, limited experimental and spectral data, and crystallographic data.

Electronic Supplementary Information (ESI) available: Characterizations of lignin and emulsions. See DOI: 10.1039/b000000x/

1 G. O. Wilson, J. S. Moore, S. R. White, N. R. Sottos and H. M. Andersson, *Adv. Funct. Mater.*, 2008, **18**, 44-52.
2 H. Jin, C. L. Mangun, D. S. Stradley, J. S. Moore, N. R. Sottos and S. R. White, *Polymer*, 2012, **53**, 581-587.
3 D. Y. Zhu, B. Wetzel, A. Noll, M. Z. Rong and M. Q. Zhang, *J. Mater. Chem. A*, 2013, **1**, 7191-7198.
4 H. Jin, C. L. Mangun, A. S. Griffin, J. S. Moore, N. R. Sottos and S. R. White, *Adv. Mater.*, 2014, **26**, 282-287.
5 X. K. D. Hillewaere, R. F. A. Teixeira, L.-T. T. Nguyen, J. A. Ramos, H. Rahier and F. E. Du Prez, *Adv. Funct. Mater.*, 2014, **24**, 5575-5583.
6 D. A. McIlroy, B. J. Blaiszik, M. M. Caruso, S. R. White, J. S. Moore and N. R. Sottos, *Macromolecules*, 2010, **43**, 1855-1859.
7 G. O. Wilson, J. S. Moore, S. R. White, N. R. Sottos and H. M. Andersson, *Adv. Funct. Mater.*, 2008, **18**, 44-52.
8 S. R. White, N. R. Sottos, P. H. Geubelle, J. S. Moore, M. R. Kessler, E. N. Brown, S. R. Sriram, and S. Viswanathan, *Nature*, 2001, **409**, 794-797.
9 E. V. Skorb, D. Fix, D. V. Andreeva, H. Möhwald and D. G. Shchukin, *Adv. Funct. Mater.*, 2009, **19**, 2373-2379.
10 M. F. Haase, D. O. Grigoriev, H. Mohwald and D. G. Shchukin, *Adv. Mater.*, 2012, **24**, 2429-2435.
11 S. H. Cho, S. R. White and P. V. Braun, *Adv. Mater.*, 2009, **21**, 645-649.
12 M. Huang, H. Zhang and J. Yang, *Corros. Sci.*, 2012, **65**, 561-566.
13 M. Huang and J. Yang, *J. Mater. Chem. A*, 2011, **21**, 11123-11130.
14 W. Wang, L. Xu, X. Li, Z. Lin, Y. Yang and E. An, *J. Mater. Chem. A*, 2014, **2**, 1914-1921.
15 G. Wu, J. An, D. Sun, X. Tang, Y. Xiang and J. Yang, *J. Mater. Chem. A*, 2014, **2**, 11614-11621.
16 D. G. Shchukin, *Polym. Chem.*, 2013, **4**, 4871-4877.
17 D. Sun, J. An, G. Wu and J. Yang, *J. Mater. Chem. A*, 2015, **3**, 4435-4444.
18 L. -T. T. Nguyen, X. K. D. Hillewaere, R. F. A. Teixeira, O. V. D. Berga and F. E. Du Prez, *Polym. Chem.*, 2015, **6**, 1159-1170.
19 G. Schneider and G. Decher, *Langmuir*, 2008, **24**, 1778-1789.
20 K. Katagiri, K. Koumoto, S. Iseya, M. Sakai, A. Matsuda, and F. Caruso, *Chem. Mater.*, 2009, **21**, 195-197.
21 Y. Wu, Q. Lai, S. Lai, J. Wu, W. Wang and Z. Yuan, *Colloid Surf. B*, 2014, **118**, 298-305.
22 K. S. Kim and S. J. Park, *Colloid Surf. B*, 2012, **92**, 240-245.
23 D. Saihi, I. Vroman, S. Giraud and S. Bourbigot, *React. Funct. Polym.*, 2005, **64**, 127-138.

24 H. Zhang, D. Liu, M. A. Shahbazi, E. Makila, B. Herranz-Blanco, J. Salonen, J. Hirvonen and H. A. Santos, *Adv. Mater.*, 2014, **26**, 4497-4503.
25 I. Polenz, D. A. Weitz and J. C. Baret, *Langmuir*, 2015, **31**, 1127-1134.
26 L. R. Arriaga, S. S. Datta, S. H. Kim, E. Amstad, T. E. Kodger, F. Monroy and D. A. Weitz, *Small*, 2014, **10**, 950-956.
27 I. Polenz, S. S. Datta and D. A. Weitz, *Langmuir*, 2014, **30**, 13405-13410.
28 J. Yang, M. W. Keller, J. S. Moore, S. R. White, and N. R. Sottos, *Macromolecules*, 2008, **41**, 9650-9655.
29 W. Wang, L. Xu, F. Liu, X. Li and L. Xing, *J. Mater. Chem. A*, 2013, **1**, 776-782.
30 B. Di Credico, M. Levi and S. Turri, *Eur. Polym. J.*, 2013, **49**, 2467-2476.
31 Y. Zhang, X. Zheng, H. Wang and Q. Du, *J. Mater. Chem. A*. 2014, **2**, 5304-5314.
32 Y. Hu, Y. Yang, Y. Ning, C. Wang and Z. Tong, *Colloid Surf. B*, 2013, **112**, 96-102.
33 X. Zheng, Y. Zhang, H. Wang and Q. Du, *Macromolecules*, 2014, **47**, 6847-6855.
34 G. Yin, Z. Zheng, H. Wang, Q. Du and H. Zhang, *J. Colloid Interface Sci*., 2014, **426**, 137-144.
35 S. Zou, Y. Hu and C. Wang, *Macromol. Rapid Commun.*, 2014, **35**, 1414-1418.
36 Y. Yang, C. Wang and Z. Tong, *RSC Adv.*, 2013, **3**, 4514-4517.
37 D. A. McIlroy, B. J. Blaiszik, M. M. Caruso, S. R. White, J. S. Moore and N. R. Sottos, *Macromolecules*, 2010, **43**, 1855-1859.
38 Z. Wei, Y. Yang, R. Yang and C. Wang, *Green Chem*., 2012, **14**, 3230-3236.
39 Y. Yang, Z. Wei, C. Wang and Z. Tong, *ACS Appl. Mater. Inter.*, 2013, **5**, 2495-2502.
40 L. Meng, Y. Yuan, M. Rong and M. Zhang, *J. Mater. Chem. A*, 2010, **20**, 6030-6038.
41 M. Zhou, Y. Liu, J. Chen and X. Yang, *J. Mater. Chem. A*, 2015, **3**, 1068-1076.
42 H. Zou, R. Wang, X. Li, X. Wang, S. Zeng, S. Ding, L. Li, Z. Zhang and S. Qiu, *J. Mater. Chem. A*, 2014, **2**, 12403-12412.
43 T. S. Skelhon, Y. Chen and S. A. F. Bon, *Soft Matter*, 2014, **10**, 7730-7735.
44 T. S. Skelhon, Y. Chen and S. A. F. Bon, *Langmuir*, 2014, **30**, 13525-13532.
45 J. Causse, A. Tokarev, J. Ravaux, M. Moloney, Y. Barré and A. Grandjean, *J. Mater. Chem. A*, 2014, **2**, 9461-9465.
46 A. R. Morgan, N. Ballard, L. A. Rochford, G. Nurumbetov, T. S. Skelhon and S. A. F. Bon, *Soft Matter*, 2013, **9**, 487-491.
47 J. Li, A. D. Hughes, T. H. Kalantar, I. J. Drake, C. J. Tucker and J. S. Moore, *ACS Macro Lett.*, 2014, **3**, 976-980.
48 D. Y. Zhu, J. W. Guo, G. S. Cao, W. L. Qiu, M. Z. Rong and M. Q. Zhang, *J. Mater. Chem. A*, 2015, **3**, 1858-1862.
49 A. R. Jones, A. Cintora, S. R. White and N. R. Sottos, *ACS Appl. Mater. Interfaces*, 2014, **6**, 6033-6039.
50 J. F. Patrick, K. R. Hart, B. P. Krull, C. E. Diesendruck, J. S. Moore, S. R. White and N. R. Sottos, *Adv. Mater.*, 2014, **26**, 4302-4308.
51 G. Wu, J. An, X. Tang, Y. Xiang and J. Yang, *Adv. Funct. Mater.*, 2014, **24**, 6751-6761.
52 M. Huang and J. Yang, *Prog. Org. Coat.*, 2014, **77**, 168-175.
53 M. Huang and J. Yang, *J. Intel. Mat. Syst. Str.*, 2014, **25**, 98-106.
54 G. Li, M. Schenderlein, Y. Men, H. Möhwald and D. G. Shchukin, *Adv. Mater. Inter.*, 2015, DOI: 10.1002/admi.201300019.
55 J. Fu, T. Chen, M. Wang, N. Yang, S. Li, Y. Wang and X. Liu, *ACS Nano*, 2013, **7**, 11397-11408.
56 M. Wang, M. Liu and J. Fu, *J. Mater. Chem. A*, 2015, **3**, 6423-6431.
57 S. Neuser, P. W. Chen, A. R. Studart and V. Michaud, *Adv. Eng. Mater.*, 2014, **16**, 581-587.

A table of contents entry

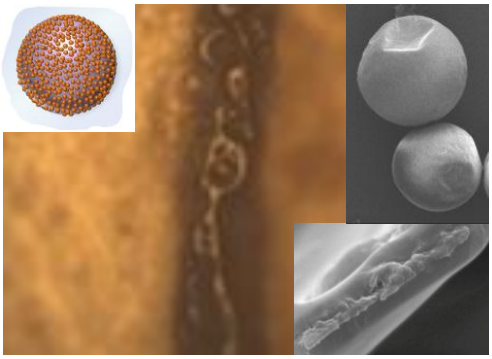

Multilayer composite microcapsules with IPDI prepared from lignin-stabilized Pickering emulsions were used for self-healing epoxy coatings.